International Journal of Engineering

Journal Homepage: www.ije.ir

Investigation on Formability of Tailor-Welded Blanks in Incremental Forming

R. Panahi liavoli, H. Gorji*, M. Bakhshi-Jooybari, M. J. Mirnia

Advanced Material Forming Research Center, Faculty of Mechanical Engineering, Babol Noshirvani University of Technology, Babol, Iran

P A P E R I N F O

Paper history:
Received 27 January 2020
Received in revised form 25 February 2020
Accepted 06 March 2020

Keywords:
Finite Element Simulation
Single Point Incremental Forming
Tailor-Welded Blanks
Welding Zone

A B S T R A C T

Steel laser tailor-welded blanks (TWBs) are produced by end-to-end joining of base sheets using different welding methods. In this article, the formability of laser TWBs of St12 and St14 with thicknesses of 1 mm and 1.5 in single point incremental forming process were experimentally and numerically investigated. First, the forming limit wall angle was experimentally determined for each of the base sheets. Then, SPIF of TWBs samples was carried out at the thinner sheet wall angle; 67°. For numerical investigation, the mechanical properties of the weld zone were obtained. For one combination of TWBs, the finite element (FE) simulation of incremental forming was performed by the use of ABAQUS/Explicit FE software. The simulation process was validated by comparing the results with those of experiments. Then, the effect of SPIF on thickness, stress and strain distribution of other combinations of TWBs was numerically investigated. The results showed that using the FE model, the SPIF of TWBs without performing high cost experimental tests can be properly investigated. Also, the results revealed that in steel laser TWBs with different thicknesses, the maximum and minimum principal strains are concentrated at the corners and the walls of the thinner sheet of TWBs, respectively. Hence, the maximum amount of effective strain is concentrated at the thinner side of TWBs corners and the weld zone of the two blanks. For the same reason, rupture is observed at these regions.

***doi**: 10.5829/ije.2020.33.05b.23*

1. INTRODUCTION

The application of computer aided manufacturing systems in metal forming processes has provided good opportunities for diversity development in geometrical models, rapid prototyping, decreasing weight, and final cost of parts [1]. One of such opportunities is Incremental Sheet Forming (ISF) of Tailor Welded Blanks (TWBs). TWBs are composed of two or more sheets with different thicknesses, properties, or even coatings, which are jointed to each other end-to-end, and then are finished into the final shape using one of the forming processes. The possibility of benefiting from diverse materials and properties in one sample, results in an impressive decrease in weight and cost of the product. Meanwhile, the difference in the mechanical properties and thickness of each of the sheets as well as the method of joining them, resulting appearance of problems in forming such blanks.

Incremental forming process was introduced by Matsubara [2] as a sheet metal forming technology without die. Nowadays, this method is suggested in industry for the production of a small number of products with high diversity [3].

Incremental forming process is divided into two types; Single Point Incremental Forming (SPIF) and Two Point Incremental Forming (TPIF), based on the way the sheets are contacted by the tool. The required equipment in this process include a simple tool with a spherical head, a fixture which is for holding the blank, and a 3-axis CNC milling machine. In this process, first the sheet is fixed by using a special fixture. Then, it is gradually shaped into the considered geometry by moving the spherical-head tool on a CNC machine in a predefined path [4]. In order to improve the dimensional accuracy, a backing plate is placed under the blank, and a blank holder is placed above it. The sheet edges are controlled by the blank holder. In SPIF method, there is nothing under the sheet, the forming is done without chipping, and it is performed through local pressure inserted from the tool on the sheet [5]. The material flow is controlled through the tool movement, and TWBs behavior in SPIF is totally

*Corresponding Author Institutional Email: *hamidgorji@nit.ac.ir* (H. Gorji)

Please cite this article as: R. Panahi liavoli, H. Gorji, M. Bakhshi-Jooybari, M. J. Mirnia, Investigation on Formability of Tailor-Welded Blanks in Incremental Forming, International Journal of Engineering (IJE), IJE TRANSACTIONS B: Applications Vol. 33, No. 5, (May 2020) 906-915

different from what happened in other traditional processes [6].

Kim and Park [7] studied the process parameters of aluminum sheet formability by SPIF process. They showed that the degree of formability in this process is higher than other common forming processes. Seong et al. [8] showed that changing the state of minimum and maximum main stresses along the sheet thickness results in the prevention of necking increasing the formability of AA 6022-T4E32 blank in SPIF. Korra et al. [9] investigated the formability of the extra-deep drawing steel sheet in SPIF. By the use of variable wall angles, the maximum fracture angle was obtained as 75.27^{o}. Daflou et al. [10] increased the stages of SPIF for the one-piece sheet blank of AA 3103 and concluded that reaching a wall angle of 90^{o} is not impossible. Ambrogio et al. [11] introduced an inverse and two-stage SPIF-based strategy; and by using statistical analysis, they performed some research about the effect of process parameters on dimensional accuracy of 1050-O aluminum alloy, 5754-H22 aluminum alloy, and DC04 deep drawing steel materials. Investigations conducted by Mirnia and Shamsari [12] showed through the use of modified Mohr-Coulomb model in numerical prediction of ductile fracture in SPIF of AA6061-T6 aluminum sheet, that the state of stress and strain in SPIF is severely non-linear; which can increase the formability in this method to values higher than other forming methods.

A number of researches has also been performed on the SPIF of TWBs. Ciubotariu and Brabie [13] explained that how the quality and position of the weld line have the maximum effect on the formability of TWBs in the mechanical tensile test of two types of steel. Ebrahimzadeh et al. [14] studied the formability of aluminum friction stir welding (FSW) blanks in TPIF process. Added to comparing SPIF and TPIF for FSW, they concluded that the formability of TPIF process was about 40% higher than SPIF. Fazli et al. [15] studied the formability of 5083 aluminum alloy blanks joined by friction stir welding in SPIF. They concluded that the FSW process did not have any negative effect on the formability, and that the forming limit angle of FSW blanks was not much different from the base sheet. Safdarian Korouyeh et al. [16] investigated the effect of laser-welding parameters on forming properties and weld line movement in TWBs by the use of Hacker test. A new analytical method for the prediction of weld line movement in TWBs was developed by Abbasi et al. [17]. Silva et al. [18] studied SPIF of TWBs made from AA1050-H111 sheets, produced by the use of FSW. The results obtained by these authors confirmed that SPIF of FSW blanks brings about the possibility of producing complex metal parts with high formability potentials. Rattnachan et al. [6] performed an investigation on the formability of TWBs blanks produced from the two materials St37 and SUS304 in SPIF. The purpose of their study was to investigate the formability of TWBs at weld zone for forming semi-circle samples. Raut et al. [19] carried out a numerical investigation on SPIF of TWBs and concluded that the maximum value of von Mises stress and equivalent plastic strain is found at the corner of the component being formed during the SPIF process. The TWBs in their study were made from AA554 and AA0552 using FSW technique.

A lot of researches have been done on incremental forming of single layer sheets; however, only a few pieces of research works have been performed on the formability and simulation of TWBs in SPIF. In the most studies which were carried out on TWBs during SPIF, the TWBs were produced by FSW. The SPIF of steel laser TWBs had not been much investigated by the researchers yet. Meanwhile, the results of studies on SPIF of one-piece sheet blanks are not applicable to SPIF of TWBs [20]. Therefore, the necessity of investigating the TWBs is sensed strongly. Because of the high costs and expensive facilities involved in experimental investigation of TWBs formability in SPIF process, the formability of more TWBs combination in SPIF process has been more examined by numerical simulation. In the present study, the formability of base sheets and also the laser TWBs, defining the mechanical properties of the weld zone and the effect of weld line direction, blank material and sheet thickness on stress, strain and thickness distribution will be investigated experimentally as well as by FE simulation. The deformation mechanism at different directions of laser TWBs has not been yet examined, which is the objective of this paper.

2. EXPERIMENTAL PROCEDURE

2. 1. Preparation of Base Sheets and Tailor-Welded Blanks The base sheets used for the experiments, are made from St12 and St14 steels with thicknesses of 1 mm and 1.5 mm. All the base sheets were one-piece sheet blanks. In order to prepare TWBs, the two base sheets must be welded end-to-end which has several combinations regarding the weld line direction relative to the rolling direction (Rd) and the thicknesses of the sheets; three of which are presented in Figure 1.

For joining the two sheets to prepare TWBs, a Nd:YAG pulsed-laser welding machine was used. The machine has the capability to enter the welding parameters digitally. The appropriate welding parameters, shown in Table 1, were obtained based on the experience of the technicians, the available data from the literature, and through trial and errors performed. Using the two materials and the two thicknesses, three total categories and ten different combinations, shown in Table 2, are considered for preparing TWBs without consideration of weld line directions. For each combination, three directions with a difference of 45^{o}

were performed for the welding line relative to the rolling direction of the base plate. In this study, the welding line along rolling direction, perpendicular to the rolling direction, and along 45° relative to the rolling direction have been examined. The three prepared samples of laser TWBs are presented in Figure 2.

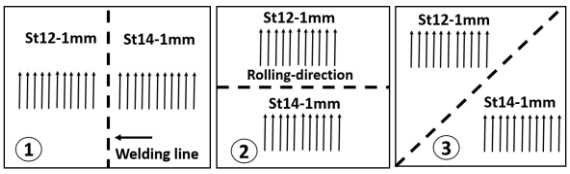

Figure 1. Three different welding lines relative to the rolling direction of the base plates and the thicknesses of the sheets

TABLE 1. Different laser-weld parameters in TWBs formation

Thickness	Parameter			
	Current (A)	Pulse width (ms)	Frequency (Hz)	Feed (mm/s)
1mm-1mm	130	6	18	5. 6
1.5mm-1.5mm	140	9	10	3.1
1mm-1.5mm	130	6	18	5.6

TABLE 2. Different combinations of St12 and St14 sheets with two thicknesses of 1mm and 1.5mm

No	Categories	Combination
1	St12-St12	St12/1-St12/1
2		St12/1.5-St12/1.5
3		St12/1-St12/1.5
4	St14-St14	St14/1-St14/1
5		St14/1.5-St14/1.5
6		St14/1-St14/1.5
7	St12-St14	St12/1-St14/1
8		St12/1.5-St14/1.5
9		St12/1-St14/1.5
10		St12/1.5-St14/1

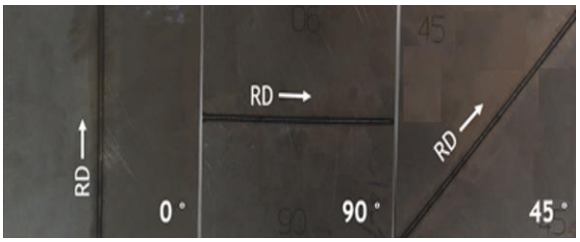

Figure 2. Three TWBs samples, the weld line is in rolling direction, perpendicular and with 45^0 to rolling direction

2. 2. SPIF of Base Sheet and Laser Tailor-Welded Blanks The experimental tests include SPIF of base sheets and TWBs for forming parts in the shape of truncated square pyramids with a larger base edge of 100 mm, a smaller base edge of 16 mm, and with a constant wall angle. In order to perform SPIF for a one-piece sheet blank, square blanks with the side dimension of 210 mm, proper for the fixture dimensions, were cut and then put on the blank holder fixture. The tool used in this study is a spherical-head tool, presented in Figure 3, is made of tungsten carbide. The needed equipment, final shape and the tool moving path for the experiments are presented in Figures 4 and 5, respectively. The movement has been performed by the use of the Powermill software as spiral movement with a vertical step of 0.5 mm. In all the experiments, the tool feed rate was kept constant as 1200 mm/min and the spindle speed was selected as 300 rpm. In order to decrease the friction between the tool and the sheet, ASE60 hydraulic oil has been applied. To obtain the forming limit angle of the base sheet, preliminary SPIF tests were performed on the truncated pyramid samples for the wall angle range between 60^0 and 71^0, and it was concluded that the most appropriate angle is 67^o. Therefore, all the examinations in this research were performed at this fixed angle. In each test, the sheet was formed upon rupture and at this moment, the rupture depth was recorded. The largest wall angle of the truncated pyramid, in which the sheet is completely formed, has been assumed as forming limit angle of the sheet. To examine the thickness distribution numerically and experimentally, two different paths were selected. Path 1 (Path 90^0) starts from the center of the smaller base

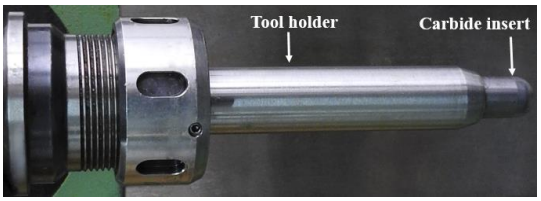

Figure 3. Spherical-head tool made of tungsten carbide, mounted on the blank holder and spindle

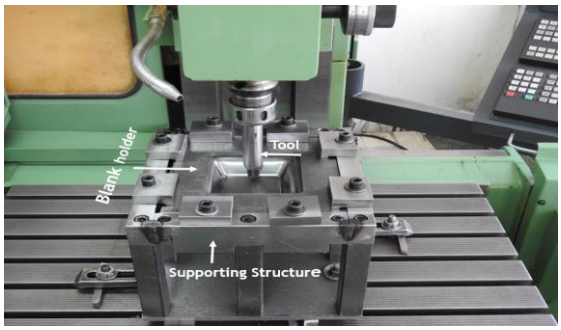

Figure 4. Required equipment for the truncated pyramid SPIF process

and ends till the middle of the larger base edge. Path 2 (Path 45^0) starts from the center of the smaller base and ends to the corner of the larger base edge (Figure 6). The formed samples were cut along the two paths using a wire cut machine. The measurement of the thickness of the sheets along the cut paths was performed using a mechanical thickness gauge with the precision of 0.01 mm. In order to define the mechanical properties of the base metal, a simple tensile test has been done according to ASTM-E08. The stress-strain curves of the base metals are presented in Figure 7.

2. 3. Finite Element Simulation

2. 3. 1. Finite Element Simulation of the Base Sheets In order to simulate SPIF process of the base sheets, the mechanical properties of the sheets should be defined. The true stress-strain curves of the base metals, shown in Figure 7, have been introduced as Hollomon power law, Equation (1). In this equation, σ is the stress of the base metal, K is the strength coefficient, ε is the uniform longitudinal strain, and n is the work hardening exponent. The mechanical properties of the materials were assigned as Table 3.

$$\sigma = K\varepsilon^n \quad (1)$$

In the current study, the forming process is simulated using ABAQUS/explicit commercial software. The spherical-head tool was considered as 3D analytical rigid, and the backing plate and blank holder as discrete rigid. Since the blank holder did not have any deformation, therefore, has not been modeled. The steel sheets were considered as deformable and that obey Von Mises yield criterion. The sheet was meshed by S4R shell elements with the size of 1 mm. The mesh sensitivity analysis was performed and is shown in Figure 8. As shown in this figure, the equivalent plastic strain corresponding to the mesh size of 0. 5, 0.75 and 1 are almost similar. In the experimental SPIF process, the edges of the sheet were fixed with a blank holder and did not have any movement or rotation. Therefore, as the boundary condition in the simulation of the process, the edges of the sheet were considered to be fixed.

The real experimental CNC program was used to generate the tool path in the simulation. Feed rate, spindle speed, vertical step down, diameter of the tool and component size were those of the experiments. By the use of the program written in MATLAB software, the CNC

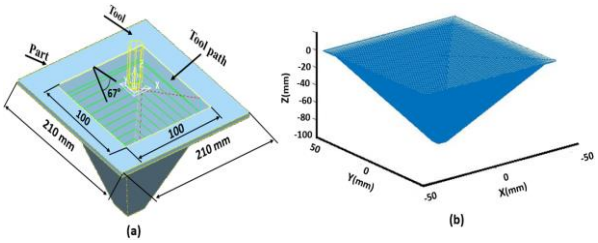

Figure 5. a) The geometry of the produced sample, b) the tool path in truncated pyramid SPIF process

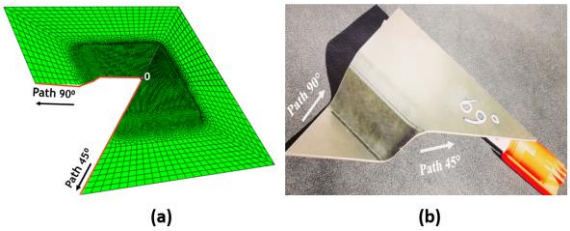

Figure 6. Cut paths of the samples formed by SPIF, a) The FEM sample, b) The experimental sample

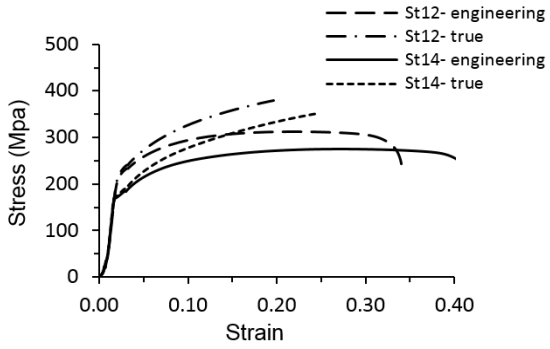

Figure 7. True and engineering stress-strain curves of the base sheets

TABLE 3. Mechanical properties of the base sheets

Sheet	St12	St14
Density (kg/m3)	7830	7830
Young modulus (GPa)	210	210
Yield strength (GPa)	220	174
Ultimate tensile strength (MPa)	311	280
Poisson ratio	0.32	0.33
Work hardening exponent (n)	0.25	0.28
Strength coefficient (K) (MPa)	524	573
Elongation	40%	45%

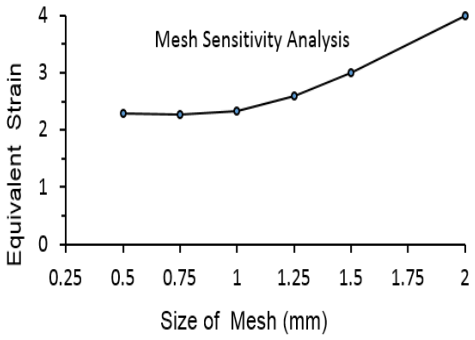

Figure 8. The mesh sensitivity diagram

program is converted into an excel file with x, y, and z coordinates of the tool movement with respect to time. These coordinates were applied to the tool in three dimensions as boundary conditions in ABAQUS. Since in this research a cooling hydraulic oil (SAE60) was used, therefore it was assumed that the temperature condition is stable and that the effect of heat is not considerable. The results reported in literature [13] showed that the tool speed does not have a significant effect on friction condition. The contact between the tool surface and the sheet was defined as the surface contact (explicit) with the penalty behavior and with the coefficient of friction of 0.2 [21]. In order to decrease the simulation time, the mass scale was used in such a way that the kinetic energy would always be insignificant relative to the internal energy during simulation. In the simulations, the middle of the sheet that largely deforms, was finely meshed, and the around of the sheet was meshed with coarse elements.

2. 3. 2. Finite Element Simulation of SPIF of TWBs

In this section, the materials St12 and St14 with different thicknesses, are considered to be jointed by laser. In order to simulate SPIF process of TWBs, firstly, the mechanical properties of weld zone should be obtained. Due to the small size of the weld cross section, preparation of the tensile test sample from the laser-weld zone is not possible [22]. One solution to this problem is the use of analytical methods for force equilibrium at the cross section of the tensile test sample made from TWBs, which estimates the mechanical properties of the weld zone. This rule, which is known as the rule of mixtures, is mainly used for samples with longitudinal welds, and it is assumed that the longitudinal strain along the base and weld metals is totally uniform [23]. The applied force on the cross section of the tensile test sample from TWBs between base metals 1 and 2, and weld zone is represented as equation 2. In this equation, P is the total force inserted on the weld section, base metal 1 and base metal 2. σ1 and σ2 are, respectively, the stresses inserted on base metals 1 and 2, A1 and A2 are the cross sectional area of base metals 1 and 2, respectively; $\bar{\sigma}_w$ is the inserted stress on the weld section, and A_w is the weld zone cross sectional area.

$$P = \sigma_1 A_1 + \sigma_2 A_2 + \bar{\sigma}_w A_w \quad (2)$$

The plain tensile test sample of TWBs and its cross section are presented in Figure 9. In the preliminary tests performed by the authors, it was realized that the St14 steel sheets did not have any anisotropy. The St12 sheets had some minor anisotropy that was negligible. Therefore, it was assumed that the base sheets and the weld zone are isotropic and obey Holloman law. By having work-hardening exponent, strength coefficient, cross-sectional area of the base metals and the weld zone, the average stress of the weld zone, $\bar{\sigma}_w$, is obtained from

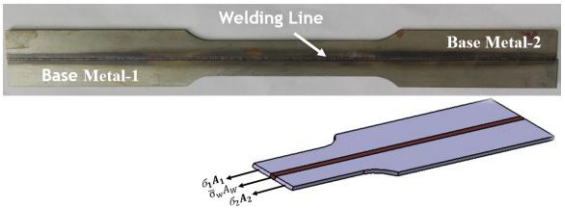

Figure 9. The cross section of base metals and weld zone in the tensile test sample from laser tailor-welded blanks

Equation 3. In this equation ε is the uniform longitudinal strain, n_i is work hardening exponent, K_i is strength coefficient, and A_i is the base sheet cross sectional area (i=1, 2). A_w is the cross sectional area of the laser weld which was calculated by the use of a profile projector. By the use of the true longitudinal strain which is obtained from tensile test, and also the average true stress which is obtained from Equation 3, the true stress-strain curve of the weld zone is obtained. This stress-strain curve obtained from the tensile test, is acceptable up to the necking point because of being uniaxial. For higher strains that occur in SPIF, extrapolation should be performed. The extrapolated plot of the weld zone with n = 0.28 and K= 610 MPa is presented in Figure 10. In order to apply different mechanical properties of weld zone, St12 and St14 sheets and by considering the thickness of the two base sheets in SPIF simulation process of TWBs, the laser TWBs is divided into three zones; the base sheet with a lower thickness, the base sheet with a higher thickness, and the weld line; the Properties and thicknesses of each zone must be inserted into the software. The designed model for SPIF simulation of TWBs is presented in Figure 11. The sample size in the simulation is the same as that in the experimental SPIF that was shown in Figure 6. After verifying the SPIF simulation of TWBs, the effects of weld line direction relative to rolling direction, the distribution of thickness, strain and stress of the formed samples are investigated.

$$\bar{\sigma}_w = \frac{P - K_1 \varepsilon^{n_1} A_1 - K_2 \varepsilon^{n_2} A_2}{A_w} \quad (3)$$

3. RESULTS AND DISCUSSION

3. 1. Experimental Results of Incremental Forming of the Base Sheet Considering the performed experiments, it has been observed that by incremental increase in the wall angle to about 67^o and 67.5^o respectively for St12 and St14 sheets with the thickness of 1 mm, the parts were successfully formed. However, after the mentioned angles, the sheets ruptured at a depth lower than the designed depth. In order to investigate the repeatability of the experiments and to make sure that SPIF of the base metals is correctly

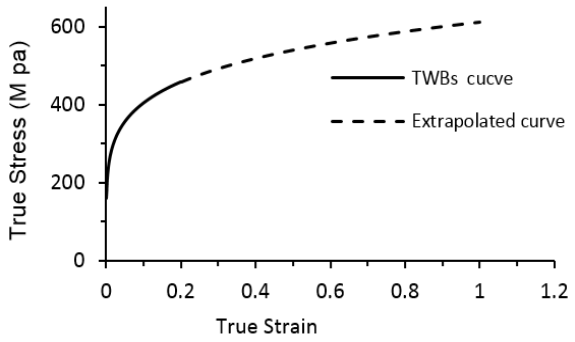

Figure 10. Extrapolated stress-strain curve of the weld zone

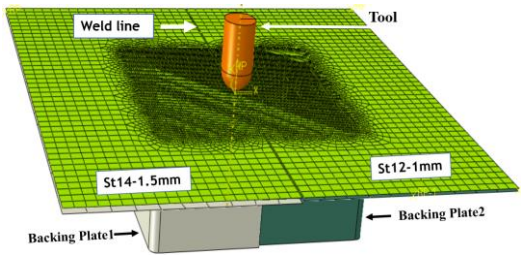

Figure 11. SPIF finite element model of truncated pyramid from TWBs

performed, a number of samples were formed from the base sheet St12 with similar conditions to the same depth of 16 mm in the form of a truncated pyramid with a wall angle of 67°. The diagrams of thickness distribution for all three samples, along 45° direction are presented in Figure 12. The difference between the minimum thicknesses of the three samples is less than 0.03 mm, which shows the repeatability of the process.

3. 2. Numerical Results of Incremental Forming of the Base Metal Simulation of SPIF process of the St12 base metal was performed according to the experimental conditions and to the same depth of 16 mm in order to form samples into a truncated pyramid shape with a wall angle of 67°. The obtained thickness distribution curves were investigated for paths 45° and 90°. Figure 13 shows the minimum thickness obtained from the simulation at the depth of 16 mm, which is about 0.33mm. In order to verify the simulation results, the obtained experimental results were used. In Figure 14, the thickness distribution curves of the three experimental samples were compared with the numerical thickness distribution curves at the depth of 16 mm and along path 90°. The maximum difference between the results is less than 0.03mm, which is about 6%.

3. 3. Experimental Results of Incremental Forming of TWBs In order to experimentally investigate the formability of laser TWBs, samples were shaped into the truncated pyramid from the TWBs along

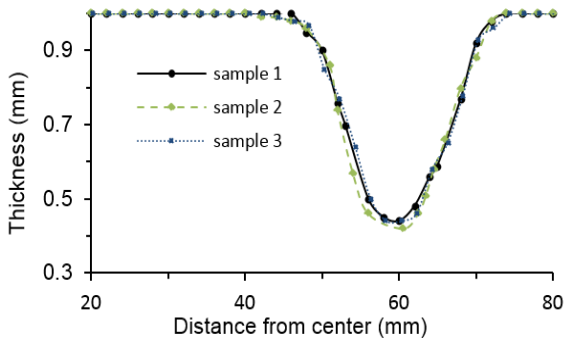

Figure 12. Experimental thickness distribution curves of SPIF samples from St12-1mm base sheet, at a depth of 16 mm, with a 45° cutting direction

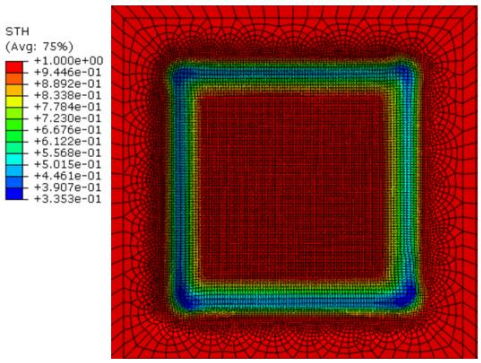

Figure 13. Minimum thickness of the formed sample to a depth of 16 mm from St12-1mm in SPIF, obtained from simulation

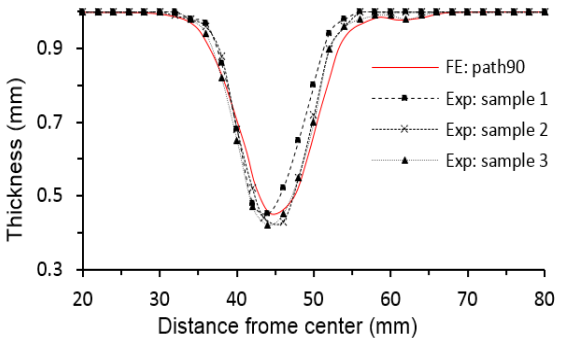

Figure 14. Experimental and numerical thickness distribution curves of the formed St12-1 base metal at the depth of 16 mm in SPIF; cutting direction 90°

three different weld line directions relative to the rolling direction. Forming of these samples was performed in the range of forming limit wall angle obtained for the sheet with lower strength, meaning 67°. Several samples of the SPIF TWBs parts are presented in Figure 15.

In order to assess the repeatability of the process and to make sure that SPIF experiments of TWBs have been carried out correctly, three samples of the blanks with

weld lines along rolling direction and with the same conditions were formed to a depth of 11 mm. The formed samples were cut along the weld line which are shown in Figure 16. The diagrams of thickness distribution along the weld line for the three samples are presented in Figure 17. The diagram of the average rupture depth of TWBs St12/1-St12/1 with weld line along 0^{o}, 45^{o} and 90^{o} is shown in Figure 18. The rupture depth of the TWBs for the 0^{o} weld line is the maximum and that for 45^{o} is the minimum value. Figure 19 shows the deformed St12-1mm+St14-1.5mm TWBs at the depth of 17 mm, in which the locations of the rupture are illustrated.

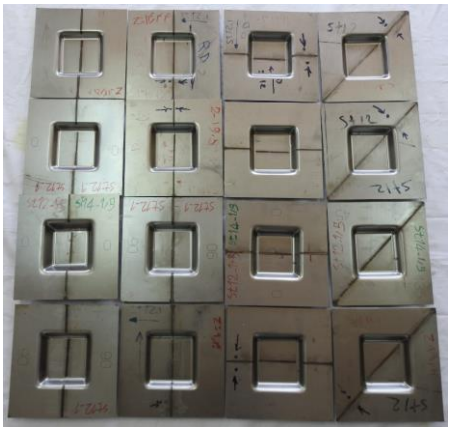

Figure 15. SPIF of TWBs made from St12 and St14 sheets with different thicknesses along three weld line directions

Figure 16. Three samples of TWBs of St12/1-St12/1 formed to a depth of 11 mm; the weld line is along rolling direction

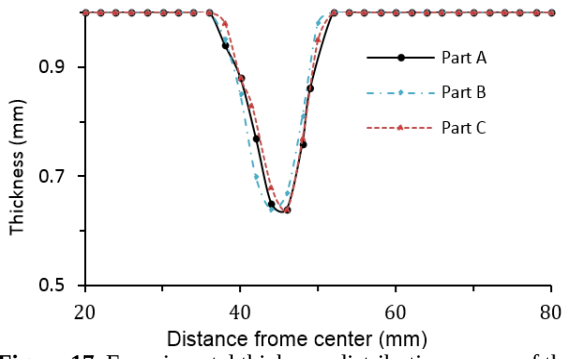

Figure 17. Experimental thickness distribution curves of the three samples of St12/1-St12/1 TBWs along rolling direction and at the depth of 11mm, for the path 90^{o}

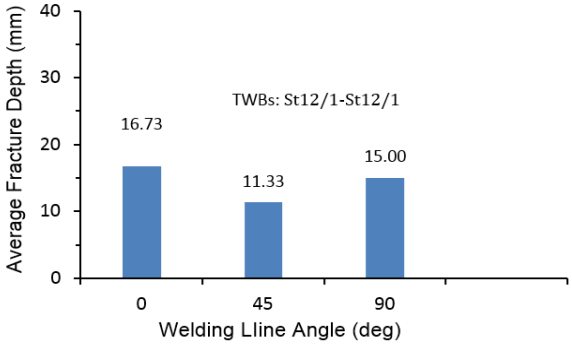

Figure 18. Rupture depth of the St12/1-St12/1 TWBs with the weld line in the direction of 0^{o}, 45^{o} and 90^{o} in experiments

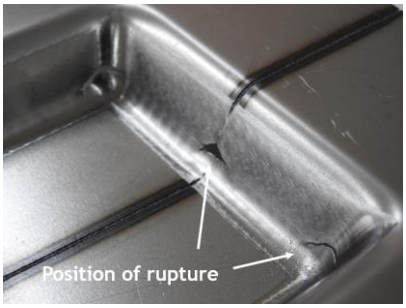

Figure 19. Rupture locations in the deformed St12-1mm+St14-1.5mm TWBs, at the depth of 17mm

3. 4. Numerical Results of Incremental Forming of TWBs Simulation of SPIF of TWBs with a weld line along the rolling direction for forming a sample in the shape of a truncated pyramid and with a wall angle of 67^{o} to a depth of 11 mm was performed. In order to verify the simulation results, thickness distribution diagrams of the three experimental samples and the numerically simulated sample to a depth of 11 mm from St12/1-St12/1 TWBs are compared in Figure 20. The weld line is along rolling direction and cutting has been done along the weld line. The minimum thickness obtained from the three experiments is about 0.64 mm and what obtained from the simulation is about 0.61 mm. The difference between the experimental and simulation results is less than 5%, which verifies the accuracy of the simulation. In order to investigate the effect of other weld line directions in forming parts into the shape of a truncated pyramid, the simulation of the part along a weld line with 45^{o} relative to the rolling direction has been performed. The thickness distribution diagrams obtained from simulation of the weld zone for the three TWBs with three different weld line directions of 0^{o}, 45^{o} and 90^{o}, and the depth of 11 mm are compared in Figure 21. Considering the results obtained from numerical analysis, when the weld line is along the rolling direction, the minimum amount of thinning is present; and, when

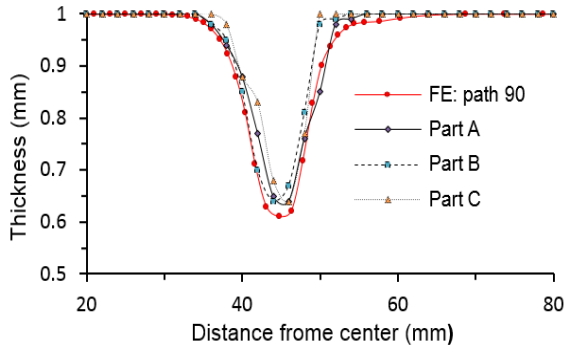

Figure 20. Experimental and numerical thickness distribution curves of the formed samples at the depth of 11mm and in rolling direction from St12/1-St12/1 TWBs in SPIF process

p

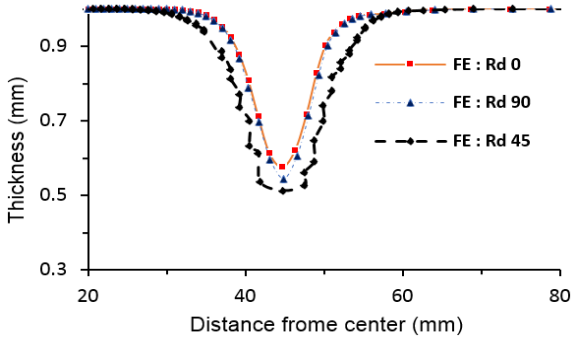

Figure 21. Numerical thickness distribution from the weld section of SPIF sample to a depth of 11 mm from St12/1-St12/1 TWBs in three directions of 0^{o}, 45^{o} and 90^{o}

the weld line is along 45^{o}, the maximum amount of thinning occurs. So, the numerical method can be considered as a suitable method for predicting thickness distribution of truncated pyramids from TWBs. Also, the rule of mixtures used in this investigation can be considered as a suitable method for obtaining the plastic properties of the laser-weld zone.

Thickness, stress, and strain distribution in SPIF of other TWBs at different fracture depths can be investigated by the use of the verified FE model. As an example, the thickness, stress, and strain distribution obtained from SPIF of TWBs for St12-1mm and St14-2 mm at the depth of 14 mm and along rolling direction are investigated. The results illustrated in this section relates to St12-1mm+St14-2 mm TWBs. It was realized that for other cases similar results were obtained that are not reported in the paper. Thickness strain distribution of St12-1+St14-2 TWBs after SPIF with the shape of a truncated pyramid with a wall angle of 67^{o} is presented in Figure 22. As it is shown in the figure, thinning of the sheet with the lower thickness is more observable, and the possibility of rupture of this compound at the corners is higher than other points. Distribution of the maximum principal strain in the formed samples at the depth of 14 mm and in rolling direction with the compound of St12-1+St14-2 and also for the base metal St12-1, is presented in Figure 23. As it is evident, at this depth, the maximum strain is about 0.95 on the walls of St12-1mm side of TWB combination, which is the thinner sheet (Figure 23a). It should be noted that, at this depth, the maximum

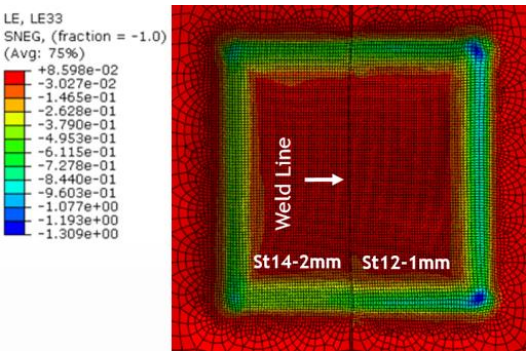

Figure 22. Thickness strain distribution to a depth of 14 mm from the tailor-welded blank (St12-1+St14-2), along rolling direction

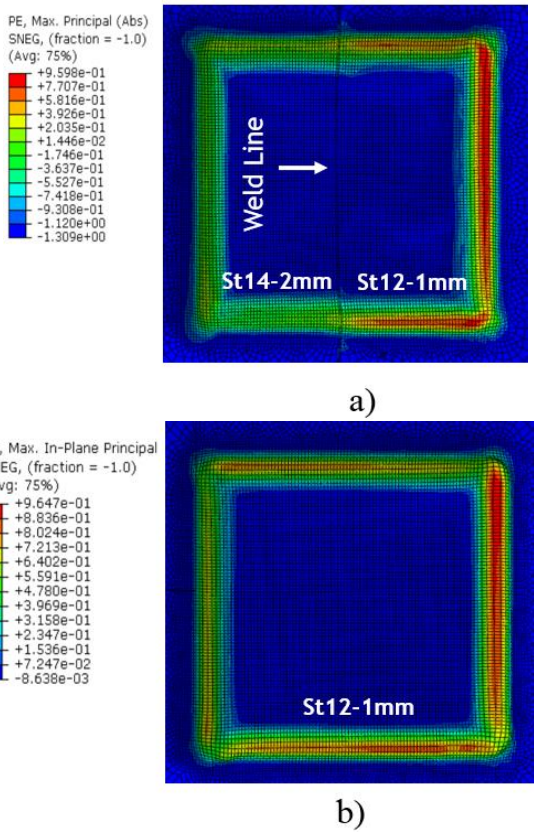

Figure 23. Maximum principal stain distribution of the formed part to a depth of 14 mm from the tailor-welded blank in SPIF, along rolling direction, a) St12-1+St14-2, b) St12-1mm

strain is about 0.96 on the walls of St12-1mm sheet (Figure 23b). Therefore, laser welding before SPIF process does not result in non-uniformity of strain distribution in samples with different thicknesses. Also, distribution of effective strains obtained from simulation of the formed sample to a depth of 14 mm from the TWBs (St12-1+St14-2) and base metal St12-1mm in SPIF process has been presented in Figure 24. Considering the fact that SPIF is a high strain process, the effective strain at the corners of the thinner sheet and at the welded region of the two sheets are higher than other points. This is in agreement with the results reported in literature [16]. As shown in Figure 24a, the maximum strain at the corner of the thinner sheet reaches 2.87 which states the rupture possibility of TWBs at these points. In contrast, at this depth, the effective strain for St12-1mm base metal is mainly observed at the wall points reaching 2.41 (Figure 24b). At this depth the prediction of rupture location by simulation was the same as in the experimental result. From this aspect, there is a conformity between the experimental and numerical results of the present study. The simulations were also done for TWBs combinations of Table 2.

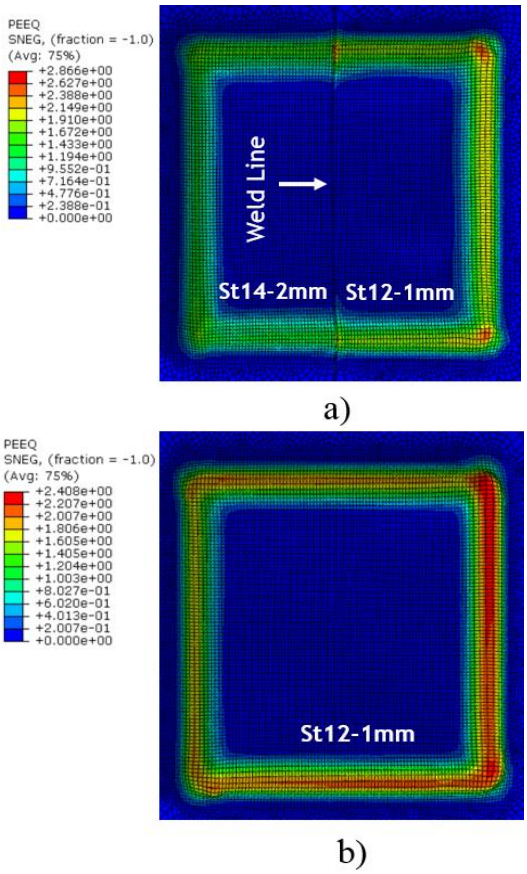

Figure 24. Effective stain distribution of the formed part to a depth of 14mm from the tailor-welded blank in SPIF, $Rd0^0$ a) St12-1+St14-2, b) St12-1mm

It was realized that the results of the simulations were generally similar. As shown in Figures 22 and 23, in SPIF process, the tool forms the sheet incrementally. Therefore, the sheet properties may not be exactly the same and some minor differences many exist in the two sides of TWBs. Some researchers reported that during SPIF of TWBs, the weld line will be shifted toward one side of TWBs [16, 19], but the in the present study, as can be seen from Figures 19, 22, 23a, and 24a, it is shown that in SPIF of laser TWBs, there is no weld line movement.

4. CONCLUTION

In this study, the formability of TWBs made from St12 and St14 sheets with thicknesses of 1 mm and 1.5 mm in SPIF of truncated pyramid parts has been numerically and experimentally investigated. By performing experiments, it was realized that the forming limit angle of TWBs is much lower, in comparison with the base metals. Through obtaining the forming limit angle for each of the base metals, and in order to prevent high costs of laser welding, forming and simulation of TWBs were only performed at the forming limit angle of the base metal with a lower strength, which was about 67°. The difference between the experimental and FE results in thickness distribution was less than 0.03mm, which was about 6%. The minimum thickness of the component in the direction of 45° for the weld line was lower in comparison with the weld line along rolling direction and the weld line perpendicular to the rolling direction. In TWBs of different thicknesses, the maximum and minimum principal strains are concentrated at the corners and the walls of the thinner sheet, respectively. For this reason, usually TWBs rupture takes place more often in these zones in comparison with the rest of TWBs regions. This model is still not able to determine the forming limit angle and fracture depth of TWBs that will be investigated in further works.

5. REFERENCES

1. Jeswiet, J., Micari, F., Hirt, G., Bramley, A., Duflou, J. and Allwood, J., "Asymmetric single point incremental forming of sheet metal", ***CIRP Annals***, Vol. 54, No. 2, (2005), 88–114.
2. Matsubara, S., "Incremental backward bulge forming of a sheet metal with a hemispherical head tool-a study of a numerical control forming system II", ***Journal of the Japan Society for Technology of Plasticity***, Vol. 35, No. 406, (1994), 1311–1316.
3. Hagan, E. and Jeswiet, J., "A review of conventional and modern single-point sheet metal forming methods", ***Proceedings of the Institution of Mechanical Engineers, Part B: Journal of Engineering Manufacture***, Vol. 217, No. 2, (2003), 213–225.
4. Kim, T.J. and Yang, D. Y., "Improvement of formability for the incremental sheet metal forming process", ***International Journal of Mechanical Sciences***, Vol. 42, No. 7, (2000), 1271–1286.

5. Emmens, W.C., Sebastiani, G. and van den Boogaard, A. H., "The technology of incremental sheet forming—a brief review of the history", ***Journal of Materials Processing Technology***, Vol. 210, No. 8, (2010), 981–997.
6. Rattanachan, K., Sirivedin, K. and Chungchoo, C., "Formability of tailored welded blanks in single point incremental forming process", In Advanced Materials Research (Vol. 979), Trans Tech Publications Ltd., (2014), 339–342.
7. Kim, Y.H. and Park, J. J., "Effect of process parameters on formability in incremental forming of sheet metal", ***Journal of Materials Processing Technology***, Vol. 130, (2002), 42–46.
8. Seong, D.Y., Haque, M.Z., Kim, J.B., Stoughton, T.B. and Yoon, J. W., "Suppression of necking in incremental sheet forming", ***International Journal of Solids and Structures***, Vol. 51, No. 15–16, (2014), 2840–2849.
9. Kurra, S. and Regalla, S. P., "Experimental and numerical studies on formability of extra-deep drawing steel in incremental sheet metal forming", ***Journal of Materials Research and Technology***, Vol. 3, No. 2, (2014), 158–171.
10. Duflou, J.R., Verbert, J., Belkassem, B., Gu, J., Sol, H., Henrard, C. and Habraken, A. M., "Process window enhancement for single point incremental forming through multi-step toolpaths", ***CIRP Annals***, Vol. 57, No. 1, (2008), 253–256.
11. Ambrogio, G. and Filice, L., "On the use of Back-drawing Incremental Forming (BIF) to improve geometrical accuracy in sheet metal parts", ***International Journal of Material Forming***, Vol. 5, No. 4, (2012), 269–274.
12. Mirnia, M.J. and Shamsari, M., "Numerical prediction of failure in single point incremental forming using a phenomenological ductile fracture criterion", ***Journal of Materials Processing Technology***, Vol. 244, (2017), 17–43.
13. Ciubotariu, V. and Brabie, G., "Weld line behaviour during uniaxial tensile testing of tailor welded blanks", ***Archives of Civil and Mechanical Engineering***, Vol. 11, No. 4, (2011), 811–824.
14. Ebrahimzadeh, P., Baseri, H. and Mirnia, M. J., "Formability of aluminum 5083 friction stir welded blank in two-point incremental forming process", ***Proceedings of the Institution of Mechanical Engineers, Part E: Journal of Process Mechanical Engineering***, Vol. 232, No. 2, (2018), 267–280.
15. Fazli, A., Asadi, P. and Soltanpour, M., "Experimental and numerical investigation of the formability of friction stir welded 5083 aluminum alloy sheets in single point incremental forming process", ***Modares Mechanical Engineering***, Vol. 18, No. 3, (2018), 45–55.
16. Safdarian Korouyeh, R., Naeini, H.M., Liaghat, G.H. and Kasaei, M.M., "Investigation of weld line movement in tailor welded blank forming", In Advanced Materials Research (Vol. 445), Trans Tech Publications Ltd., (2012), 39–44.
17. Abbasi, M., Hamzeloo, S.R., Ketabchi, M., Shafaat, M.A. and Bagheri, B., "Analytical method for prediction of weld line movement during stretch forming of tailor-welded blanks", ***The International Journal of Advanced Manufacturing Technology***, Vol. 73, No. 5–8, (2014), 999–1009.
18. Silva, M.B., Skjødt, M., Vilaça, P., Bay, N. and Martins, P. A. F., "Single point incremental forming of tailored blanks produced by friction stir welding", ***Journal of Materials Processing Technology***, Vol. 209, No. 2, (2009), 811–820.
19. Raut, J., Marathe, S. and Raval, H., "Numerical Investigation on Single Point Incremental Forming (SPIF) of Tailor Welded Blanks (TWBs)", In Advances in Simulation, Product Design and Development, Springer, (2020), 43–54.
20. Jackson, K. and Allwood, J., "The mechanics of incremental sheet forming", ***Journal of Materials Processing Technology***, Vol. 209, No. 3, (2009), 1158–1174.
21. Malyer, E. and Müftüoğlu, H. S., "The Influence of Friction Conditions on Formability of DC01 Steels by ISF", ***IOSR Journal of Mechanical and Civil Engineering Ver I***, Vol. 12, (2015), 134–138.
22. Rojek, J., Hyrcza-Michalska, M., Bokota, A. and Piekarska, W., "Determination of mechanical properties of the weld zone in tailor-welded blanks", ***Archives of Civil and Mechanical Engineering***, Vol. 12, No. 2, (2012), 156–162.
23. Abdullah, K., Wild, P.M., Jeswiet, J.J. and Ghasempoor, A., "Tensile testing for weld deformation properties in similar gage tailor welded blanks using the rule of mixtures", ***Journal of Materials Processing Technology***, Vol. 112, No. 1, (2001), 91–97.

Persian Abstract

چکیده

ورق‌های جوش دوخت شده لیزری فولادی از اتصال لب به لب ورق‌های پایه با استفاده از روش‌های مختلف جوشکاری تولید می‌شوند. در این مقاله، شکل‌پذیری ورق‌های ترکیبی اتصال داده شده با جوش لیزر از ورق‌های پایه St12 و St14 با ضخامت‌های ۱ و۱/۵ میلیمتر در فرآیند شکل‌دهی تدریجی تک نقطه‌ای (SPIF) به¬طور تجربی و عددی مورد بررسی قرار گرفته است. ابتدا، زاویه حد شکل‌دهی هر یک از ورق‌های پایه به روش تجربی تعیین گردید. سپس SPIF ورق‌های ترکیبی در زاویه جداره حد شکل‌دهی ورق نازک‌تر یعنی 67o درجه انجام شد. برای بررسی عددی، خواص مکانیکی منطقه جوش- دوخت شده با لیزر به¬دست آمد. شبیه سازی المان محدود فرآیند شکل‌دهی تدریجی برای یک مورد ورق ترکیبی با استفاده از نرم افزار اباکوس انجام شد. با مقایسه نتایج تجربی با عددی، فرایند شبیه‌سازی اعتبار سنجی شد. تاثیر فرایند SPIF بر روی توزیع ضخامت، تنش و کرنش برای سایر ورق‌های ترکیبی، به روش عددی مورد بررسی قرار گرفت. نتایج حاصل از این تحقیق نشان داد که با استفاده از مدل المان محدود استفاده شده در این پژوهش می‌توان به بررسی SPIF ورقهای ترکیبی پرداخت و از این طرق از هزینه های زیاد تست های تجربی جلوگیری ¬به¬عمل آورد. هم¬چنین نتایج نشان داد که در ورق‌های جوش- دوخت شده لیزری با ضخامت‌های مختلف، کرنش‌های اصلی بیشینه و کمینه به ترتیب در گوشه‌ها و دیواره‌های سمت ورق با ضخامت کمتر قرار دارند. به¬علاوه، بیشترین مقدار کرنش مؤثر در محل اتصال دو ورق و در گوشه‌های ورق نازک‌تر قطعه ترکیبی می‌باشد. از این رو، پارگی در این ناحیه نسبت به دیگر نقاط ورق ترکیبی بیشتر مشاهده می‌شود.